



HAL
open science

Optimal control techniques for thermo-acoustic tomography

Maïtine Bergounioux, Xavier Bonnefond, Pierre Maréchal

► **To cite this version:**

Maïtine Bergounioux, Xavier Bonnefond, Pierre Maréchal. Optimal control techniques for thermo-acoustic tomography. 2010. hal-00530719v2

HAL Id: hal-00530719

<https://hal.science/hal-00530719v2>

Preprint submitted on 26 May 2011

HAL is a multi-disciplinary open access archive for the deposit and dissemination of scientific research documents, whether they are published or not. The documents may come from teaching and research institutions in France or abroad, or from public or private research centers.

L'archive ouverte pluridisciplinaire **HAL**, est destinée au dépôt et à la diffusion de documents scientifiques de niveau recherche, publiés ou non, émanant des établissements d'enseignement et de recherche français ou étrangers, des laboratoires publics ou privés.

Optimal control techniques for thermo-acoustic tomography

Maitine Bergounioux*, Xavier Bonnefond† and Pierre Maréchal‡

May 21, 2011

Abstract

Thermo-acoustic and photo-acoustic tomography are imaging techniques that combine high electromagnetic absorption contrast between two media with ultrasound high resolution. Both techniques lead to an ill-posed inverse problem. One currently has a choice between three main types of reconstruction procedures namely the filtered backprojection formulae, eigenfunction expansion methods and time reversal method. In this paper we propose to investigate this inverse problem with an alternative control formulation : in our model the function to be recovered is the control function while the (acoustic) pressure is the state function which satisfies a wave equation. We stress that our objective is to give modelling hints, and not to provide new results. Otherwise expressed, the originality of this paper lies essentially in the way the problem is stated.

Keywords : Tomography, Image Processing, Control Theory

1 Introduction

Thermo-acoustic and photo-acoustic tomography are imaging techniques that combine high electromagnetic absorption contrast between two media with ultrasound high resolution. These hybrid systems use an electromagnetic pulse as an input and record ultrasound waves as an output. The electromagnetic energy is distributed at a given time as uniformly as possible through the object. The induced increase of temperature depends on the local absorption properties (for example, cancerous tissues absorb more energy than healthy ones). This opens the way to the detection of heterogeneities *via* measurements of the pressure field. Heterogeneities behave like internal acoustic sources, and the signals recorded by pressure detectors outside the medium under study provide information on their distribution. One speaks of thermo-acoustic tomography (TAT) when the heating is realized by means of microwaves, and of photo-acoustic tomography (PAT) when optical heating is used. While in TAT waves of radio frequency range are used to trigger the ultrasound signal, in the PAT the frequency lies in the visual or near infra-red ranges. In brief, TAT and PAT are two hybrid techniques using electromagnetic waves as an excitation (input) and acoustic waves as an observation (output). For the mathematical purpose there is no distinction between these methods. Both techniques lead to an ill-posed inverse problem of the same form which, under simplifying assumptions, entails inversion (in the wide sense) of the spherical Radon transform.

More precisely, the main problem can be formulated as follows [19, 20, 21]: given the sound speed $c(x)$ and measured data y_{obs} on $S \subset \mathbb{R}^n$ ($n = 2, 3$), find the initial value $u_o(x)$ of the pressure

*UMR 6628 -MAPMO, Fédération Denis-Poisson, Université d'Orléans, BP 6759, 45067 Orléans cedex, France, maitine.bergounioux@univ-orleans.fr

†Institut de Mathématiques de Toulouse, Université Paul Sabatier 31062 Toulouse cedex 9, France , xavier.bonnefond@mip.ups-tlse.fr

‡Institut de Mathématiques de Toulouse, Université Paul Sabatier 31062 Toulouse cedex 9, France , pierre.marechal@mip.ups-tlse.fr

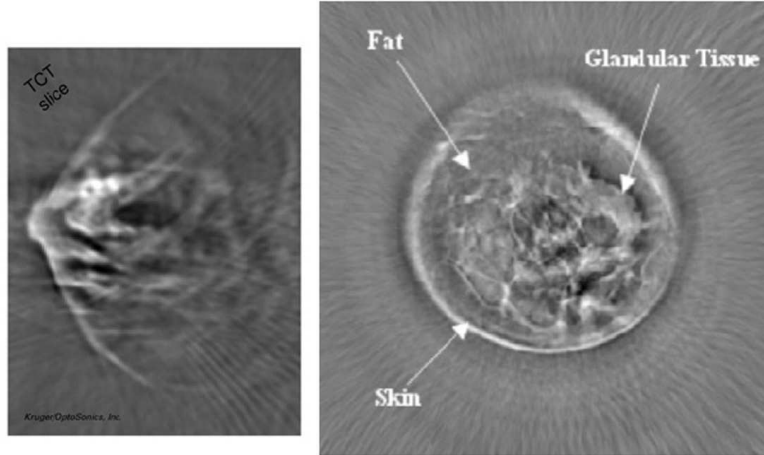


Figure 1: Realization of a tomograph with integrating transducers, from Patch and Scherzer [29]

$y(x, t)$ where y is the solution to the problem

$$\left\{ \begin{array}{l} \frac{\partial^2 y}{\partial t^2}(t, x) - c^2(x)\Delta y(t, x) = 0, \quad (t, x) \in [0, T] \times \mathbb{R}^n, \\ y(0, x) = u_o(x), \quad x \in \mathbb{R}^n, \\ \frac{\partial y}{\partial t}(0, x) = 0, \quad x \in \mathbb{R}^n, \\ y(t, x) = y_{obs}(t, x), \quad x \in S, t \in [0, T]. \end{array} \right. \quad (1)$$

We shall briefly justify this model in the sequel. The initial value u_o is the TAT (or PAT) image. This problem is highly ill-posed. In most reconstruction methods in TAT, additional assumptions are performed such as, for example, conditions on the support of the function to be recovered and/or the observation surface, or a constant sound speed. A nice overview of the state of art has been done in [21]. We summarize the introduction (for more details one can refer to the whole paper). One currently has a choice between three main types of reconstruction procedures for closed observation surfaces, namely the filtered backprojection formulae, eigenfunction expansion methods and time reversal methods.

The filtered backprojection approach is the most popular [13, 15, 16, 19, 22]. However, it is not clear that backprojection-type formulae could be written for any closed observation surface S . In [16], inversion formulae are provided assuming odd dimensions and constant sound speed. Indeed, in this case the Huygens' principle holds : for any initial source with a compact support, the wave leaves any bounded domain in a finite time. This is no longer true if the spatial dimension is even and/or the sound speed is not constant. All known formulae of filtered backprojection type assume constant sound speed and thus are not available for acoustically inhomogeneous media. In addition, the only closed bounded surface S for which such formulae are known is a sphere.

Expansion series are useful in the case where the Huyghens principle is valid. This approach was extended to the constant speed and arbitrary closed observation surface and modified by the usage of the eigenfunctions of the Laplacian with Dirichlet conditions on S [8]. It theoretically works for any closed surface and for variable sound speeds [32].

The time reversal method [20, 21] can be used for approximating the initial pressure when the sound speed inside the object is variable. It works for arbitrary geometry of the closed observation surface S . The sound speed can be variable. Ammari *et al.* [3, 4, 5, 6] have performed sharp analysis of these problems both from the modelling and numerical points of view.

In this paper we propose to investigate this inverse problem with an alternative formulation. We propose a *control* approach: in our model the function to be recovered is the control function while the pressure is the state function which satisfies a wave equation. We stress that our objective is to give modelling hints, and not to provide new results. Otherwise expressed, the originality of this paper lies essentially in the way the problem is stated.

There are many ways to define the state equation and the cost functional (observation) in the optimal control or controllability approach. We state a few open problems for future investigation, which cover various fields such as controllability theory, optimal control both from the theoretical and numerical viewpoints, the relationship between Fourier analysis and the control approach (Fourier aliasing effects and numerical approximations for the wave equation), shape optimization and so on.

The paper is organized as follows: in the next section, we present the physical problem and the model, together with the *integral* formulation (involving the spherical Radon transform). In Section 3, we present the inverse problem and usual variational techniques to address the ill-posedness. We propose an optimal control approach in section 4, present approximated and regularized models and derive general optimality conditions. In Section 5, we present simple numerical tests to compare the proposed approach to some classical methods.

2 The direct TAT model

A precise description of the physical model of TAT (or PAT) can be found in [30]. We outline here a simplified model. Let us denote by $v(x, t)$ the fluid velocity at position x and time t , and make the following physical assumptions:

1. $v(x, t)$ is small;
2. the fluid is non viscous and non turbulent;
3. there is no external force.

We also assume that the density $\rho = \rho(x, \tau)$ and pressure $p = p(x, \tau)$ undergo small variations:

$$\rho = \rho_0 + \delta\rho \quad \text{with} \quad |\delta\rho| \ll \rho_0 \quad \text{and} \quad p = p_0 + \delta p \quad \text{with} \quad |\delta p| \ll p_0.$$

This allows for linearizing the *mass conservation* and *momentum conservation equations*, which then read

$$\frac{\partial \rho}{\partial \tau} = -\rho_0 \nabla \cdot v \quad \text{and} \quad \rho_0 \frac{\partial v}{\partial \tau} = -\nabla p,$$

respectively. In the latter equations and from now on, ρ and p stand for the variations $\delta\rho$ and δp . Combining these equations yields

$$\frac{\partial^2 \rho}{\partial t^2} - \Delta p = 0. \tag{2}$$

In order to link ρ and p with the absorbed electromagnetic radiation, one makes use of the *thermal expansion equation*, whose linearized form reads

$$\frac{\partial \rho}{\partial t} = \frac{1}{c^2} \frac{\partial p}{\partial t} - \frac{\beta}{c_p} r. \tag{3}$$

Here, β , c_p and c denote respectively the thermal expansion coefficient, the specific heat capacity and the (adiabatic) speed of sound, while $r = r(x, t)$ denotes the absorbed electromagnetic power. From (2) and (3), we easily obtain

$$\left(\frac{1}{c^2} \frac{\partial^2}{\partial t^2} - \Delta \right) p = \frac{\beta}{c_p} \frac{\partial r}{\partial t}. \tag{4}$$

Now, the absorbed electromagnetic power $r(x, t)$ is related to the *absorption coefficient* $\psi = \psi(x)$ by the equation $r(x, \tau) = I(x, \tau)\psi(x)$, in which $I(x, \tau)$ is the radiation intensity. Finally, due to the high magnitude of the speed of light, one can assume that $I(x, t)$ takes the separated form $I(x) = J(x)j(t)$. Equation (4) then reads

$$\left(\frac{\partial^2}{\partial t^2} - c^2 \Delta \right) p = \frac{\beta c^2 J \psi}{c_p} \frac{\partial j}{\partial t}.$$

The function $f(x) := \frac{\beta c^2(x) J(x) \psi(x)}{c_p}$ is referred to as the *energy deposition function*. Finally, we can assume that the pressure increment, together with its time derivative, is zero at the initial time (right before illumination). We are then led to consider the following system:

$$(TAT) \begin{cases} \frac{\partial^2}{\partial t^2}(x, t) - c^2(x) \Delta p(x, t) &= f(x) \frac{\partial j}{\partial t}(t), \\ p(x, 0) &= 0, \\ \frac{\partial p}{\partial t}(x, 0) &= 0. \end{cases}$$

To simplify the problem, it is usually assumed that the sound speed c is constant (normalized to 1). An alternative formulation of the above *linear direct problem* is an integral formulation. Recall that the *direct problem* consists in determining $p(x, t)$ for all $(x, t) \in \mathbb{R}^3 \times \mathbb{R}_+$ from the knowledge of f and j . It is well known (see e.g. [19]) that the solution is given by

$$p(x, t) = \left(\frac{dj}{dt} \otimes (tRf) \right) (x, t). \quad (5)$$

Here, the *convolution* operation \otimes is defined by

$$(g \otimes h)(x, t) = \int_0^t g(t-s)h(x, s) ds$$

and the operator R , referred to as the *spherical Radon transform*, is defined by

$$(Rf)(x, t) := \frac{1}{4\pi} \int_{S^2} f(x + t\omega) d\omega.$$

In TAT, one is rather confronted to the *inverse problem*:

Recover the energy deposition function $f(x)$ from measurements of $p(x, t)$ for x over a surface S outside the illuminated fluid.

We now show that additional approximations give rise to an integral formulation of the latter inverse problem, under the assumption that the *intensity profile* $j(t)$ is nearly a Dirac centered at the origin. Assuming that j has support in $[0, T]$ (see Figure 2 (left)), one may write, for every smooth function $h(x, t)$,

$$\frac{d}{dt}(j \otimes h)(x, t) = \left(\frac{dj}{dt} \otimes h \right) (x, t).$$

If $j \approx \delta$, then $\frac{dj}{dt} \otimes h \approx \frac{dh}{dt}$, so that $\left(\frac{dj}{dt} \otimes (tRf) \right) (x, t) \approx \frac{d}{dt}(tRf)$. Consequently, Equation (5) can be approximated by

$$p(x, t) = \frac{d}{dt}(tRf). \quad (6)$$

We see that, after integrating and dividing by t , measurements of $p(x, t)$ on $S \times \mathbb{R}_+$ give access to approximate values of $(Rf)(x, t)$ on the same domain.

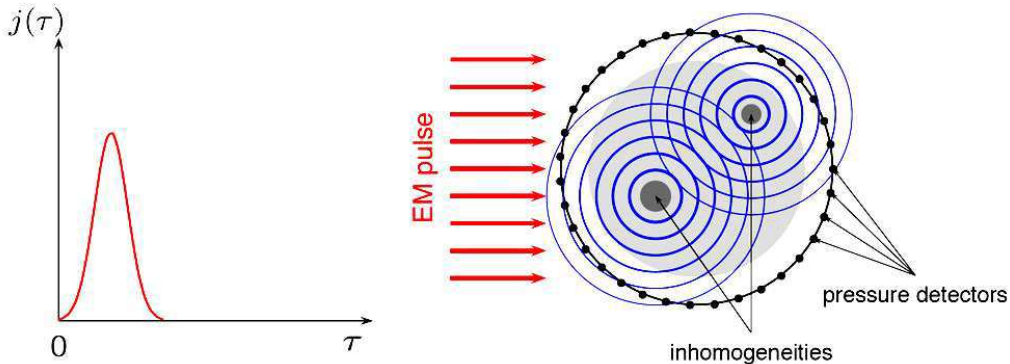


Figure 2: Physical principle of Thermo-acoustic Tomography: intensity time profile of the EM pulse (left) and scheme showing the pressure wave generation and propagation (right).

However, this integral formulation is purely *linear* and cannot be generalized to non-linear models. From the numerical point of view, the integral formulation leads to the so-called filtered back-projection method.

3 Variational techniques for the inverse problem

The integral formulation of the problem leads to a linear inverse problem of standard form, that is:

Recover f from an approximate knowledge g of Rf , where R is a compact linear operator (modelling the data acquisition process) from a norm space into another.

In TAT, R is the spherical Radon transform. As already mentioned, there are several methods to solve the inverse problem using exact or approximate formulas to estimate the inverse of R .

A classical approach to solve (ill posed) inverse problems is the least-square formulation using a regularization process (a penalization term for example) to get the well posedness. The general formulation stands

$$\min \|L(g) - A(f)\| + \alpha\mathcal{H}(f) ,$$

where g is the data and f the function to recover. We describe A , L operators thereafter and \mathcal{H} is a regularizing operator. The functional framework has to be made precise as well. In the sequel we focus on two approaches:

- The first one is the regularization by mollification which is inspired by the integral formulation : here $A = R$ (the spherical Radon transform) and the operator L is a linear operator that provides a preprocessing transformation for the data g .

We call *regularization by mollification* a set of reconstruction methodologies deriving from the idea that the original ill-posed problem of reconstructing the unknown object f should be replaced by that of recovering a smooth *version* of it. In this approach, the target object is no longer f but $\phi * f$, where ϕ is a *convolution kernel* and $*$ denotes the convolution operation.

This idea has been developed in two different ways, independently. One of them, which bears the name of *approximate inverse*, was introduced by Louis and Maaß [26, 27, 28]. In the context of TAT, it was developed by Altmeier, Schuster and Scherzer [19]. The other

way goes back to Lannes *et al.* [23], who introduced a particular *variational* regularization in the context of deconvolution and aperture synthesis. This approach was further analyzed and developed more recently by Alibaud *et al.* [1] and Bonnefond *et al.* [11] (see also [2]).

- The second approach is an optimal control approach that derives from the PDE formulation. It seems to be more general than the previous techniques since the PDE can be non linear what the integral formulation does not allow. In this case, L is the identity operator and A associates the solution $f := A(g)$ to equation (1) (with g instead of u_0) to the data g . The regularizing term $\mathcal{H}(f)$ comes from a priori knowledge of the solution f .

We first briefly present the regularization by mollification

3.1 Approximate inverses

Given a continuous and nonnegative function ϕ with $\int \phi = 1$, one defines the family

$$\phi_\beta(x, y) := \frac{1}{\beta^n} \phi\left(\frac{x-y}{\beta}\right), \quad \beta > 0,$$

called an *approximation of unity*. The mollified version of f , denoted f_β , can be expressed as the scalar product of f by $\phi_\beta(\cdot, y)$:

$$f_\beta(y) := \int f(x) \phi_\beta(x, y) dx = \langle f, \phi_\beta(\cdot, y) \rangle.$$

Now, it is well-known that, in several senses,

$$\int f(x) \phi_\beta(x, \cdot) dx \rightarrow f \quad \text{as } \beta \downarrow 0.$$

Assuming that $\phi_\beta \in \text{ran } R^*$, let ψ_β be defined by

$$\psi_\beta(\cdot, y) = (R^*)^{-1} \phi_\beta(\cdot, y). \quad (7)$$

Then, one has:

$$f_\beta(y) = \langle f, \phi_\beta(\cdot, y) \rangle = \langle f, R^* \psi_\beta(\cdot, y) \rangle = \langle Rf, \psi_\beta(\cdot, y) \rangle.$$

We see that if one can compute explicitly ψ_β , f_β is readily obtained from the data $g = Rf$ by taking the scalar product with the so-called *reconstruction kernel* ψ_β . In the case where R^* is not invertible, one may replace $(R^*)^{-1}$ in equation (7) by the pseudo-inverse of R^* (which corresponds to the least-square solution of the equation $R^* \psi(\cdot, y) = \phi_\beta(\cdot, y)$). Clearly, the difficulty in this method lies in general in equation (7) which is an ill-posed problem as well. However, as mentioned above this nice duality trick has been successfully applied in the context of TAT by Haltmeier *et al.* in [19].

3.2 Regularization by mollification

We assume here that the original object f_0 has support in a bounded domain Ω_0 in \mathbb{R}^d , and that the *mollified* object $\phi * f_0$ has *most* of its support in $\Omega \supset \Omega_0$. Notice that, if ϕ is chosen to have compact support, the definition of Ω is straightforward.

We also assume that R maps $L^2(\Omega)$ into some infinite dimensional separable Hilbert space G , and that R is compact and injective.

The convolution kernel is regarded as a member of the family

$$\phi_\beta(x) := \frac{1}{\beta^d} \phi\left(\frac{x}{\beta}\right), \quad \text{with } \phi \in L^1(\mathbb{R}^d) \quad \text{and} \quad \int_{\mathbb{R}^d} \phi(x) dx = 1. \quad (8)$$

The latter family is an *approximation of unity*, and the choice of β determines the target resolution. Clearly, in this approach, the relevant regularization parameter is β .

Let C_β denote the convolution by ϕ_β . We now aim at approximating the new *target object* $C_\beta f = \phi_\beta * f_0$, which is performed by solving the following optimization problem:

$$(\mathcal{P}_\beta) \quad \left\{ \begin{array}{l} \text{Minimize} \quad \frac{1}{2} \|\Phi_\beta g - Rf\|_G^2 + \frac{\alpha}{2} \|(I - C_\beta)f\|_{L^2}^2 \\ \text{s.t.} \quad f \in L^2(\Omega), \end{array} \right.$$

in which I denotes the identity and $\Phi_\beta: G \rightarrow G$ is itself a solution to:

$$(\mathcal{Q}_\beta) \quad \left\{ \begin{array}{l} \text{Minimize} \quad \frac{1}{2} \|RC_\beta - XR_{[E]}\|_{L(E,G)}^2 \\ \text{s.t.} \quad X \in L(G), \quad X = 0 \text{ on } (\text{ran } R_{[E]})^\perp. \end{array} \right.$$

Here, E is a subspace of $L^2(\mathbb{R}^d)$, $L(E, G)$ denotes as usual the space of continuous linear mappings from E to G and $L(G) := L(G, G)$.

The choice of the functional to be minimized in (\mathcal{P}_β) can be explained as follows. Any object f is the sum of its *low frequency component* $C_\beta f$ and of its *high frequency component* $(I - C_\beta)f$. The functional to be minimized acts on each component as independently as possible: the *fit term* introduces constraints on the low frequency component while the *regularization term* deals with the high frequency component. The complementarity of the *filters* $\hat{\phi}_\beta$ et $1 - \hat{\phi}_\beta$ allows for a smooth transition between the experimental and regularization constraints.

We emphasize that, unlike most regularization techniques, the fit term requests adequacy to the *regularized data* $\Phi_\beta g$. The rationale for this is that, in some sense, $\Phi_\beta g$ is optimally consistent with the new target object. Ideally, Φ_β should be such that

$$\Phi_\beta R = RC_\beta, \tag{9}$$

which may not be feasible. Therefore, Φ_β is chosen to minimize the discrepancy in Equation (9).

4 A control formulation

In this section, the pressure p will be denoted y , in order to fit the traditional notation in optimal control.

4.1 The state equation

We have seen in the previous section that the equation that describes the behavior of the system is (in \mathbb{R}^n with $n = 3$):

$$\left\{ \begin{array}{l} \frac{\partial^2 y}{\partial t^2}(t, x) - c^2(x)\Delta y(t, x) = u_o(x)\frac{\partial j}{\partial t}(t), \quad (t, x) \in [0, T] \times \mathbb{R}^n, \\ y(0, x) = 0, \quad x \in \mathbb{R}^n, \\ \frac{\partial y}{\partial t}(0, x) = 0, \quad x \in \mathbb{R}^n. \end{array} \right. \tag{10}$$

where j is the electromagnetic pulse intensity profile and c the sound speed.

More generally we set $u(t, x) := u_o(x)\frac{\partial j}{\partial t}(t)$. The function to be recovered u is regarded as a *control function* while the pressure y is regarded as the *state function*. Therefore Equation (10) is the so-called *state equation*.

Remark 1 *By using Duhamel's principle [13], one may rewrite this state equation as*

$$\begin{cases} \frac{\partial^2 y}{\partial t^2}(t, x) - c^2(x)\Delta y(t, x) = 0 & \text{in } [0, T] \times \mathbb{R}^n, \\ y(0, x) = u_o(x), & \text{in } \mathbb{R}^n, \\ \frac{\partial y}{\partial t}(0, x) = 0 & \text{in } \mathbb{R}^n. \end{cases} \quad (11)$$

So, in this context, the control function can be a distributed one or an initial one. However, this equivalence is only valid in the linear case and we focus on the distributed case.

Recall that, if V is a norm space endowed with $\|\cdot\|_V$, then for every $p \in [1, \infty]$

$$L^p(0, T; V) := \{y : [0, T] \times \mathbb{R}^n \rightarrow \mathbb{R} \mid y(t, \cdot) \in V \text{ a.e. } t \in (0, T) \\ \text{and } \int_0^T \|y(t, \cdot)\|_V^p dt < +\infty\}.$$

and

$$\mathcal{C}(0, T; V) := \{y : [0, T] \times \mathbb{R}^n \rightarrow \mathbb{R} \mid \forall t \in (0, T) \ y(t, \cdot) \in V \\ \text{and } t \mapsto \|y(t, \cdot)\|_V \text{ is continuous}\}.$$

The original problem domain is \mathbb{R}^n . This is consistent with the fact that one usually uses classical Fourier analysis (Radon transform, spherical means,...) since the uncertainty principle do not allow compact supports both in the time and frequency domains. The control viewpoint requires the definition of boundary conditions (to infinity if the domain is \mathbb{R}^n) to use duality methods and Green formulae. By contrast, the advantage of this approach is that we may choose an open bounded subset \mathcal{B} as the domain and use finite differences or finite elements to compute the solution. A challenging application is to set a model which allows for using both spectral (Fourier) analysis and finite difference methods.

We recall a regularity and existence abstract result which gives indication about the functional framework to be used (with appropriate regularity assumptions on c and $c \geq c_0 > 0$):

Theorem 4.1 ([25] Vol. 1 p 286) *If $u \in L^2([0, T] \times \mathbb{R}^n)$, then (10) has a unique solution in $\{y \in L^2(0, T, H^1(\mathbb{R}^n))\}$, $y_t \in L^2([0, T] \times \mathbb{R}^n)$. Moreover*

$$y \in \mathcal{C}(0, T; H^1(\mathbb{R}^n)) \text{ and } y_t \in \mathcal{C}(0, T; L^2(\mathbb{R}^n)),$$

and the solution y continuously depends on u .

In the sequel, we shall avoid using the whole space \mathbb{R}^n . Therefore, we consider that infinity means *far enough* and that the problem domain can be an open ball $\mathcal{B} \subset \mathbb{R}^n$ with large radius. Indeed the pressure y quickly vanishes and we may consider that it is equal to 0 on the boundary $\partial\mathcal{B}$ of the ball. The ball \mathcal{B} contains Ω as well as the sensors location ω_ε (we shall justify the notation later on). If we impose Dirichlet conditions on the boundary, we get:

$$\begin{cases} \frac{\partial^2 y}{\partial t^2}(t, x) - c^2(x)\Delta y(t, x) = u(t, x), & \text{in }]0, T[\times \mathcal{B} := Q, \\ y(0, x) = 0, & \text{in } \mathcal{B} \\ \frac{\partial y}{\partial t}(0, x) = 0 & \text{in } \mathcal{B} \\ y = 0 & \text{on } S \end{cases} \quad (12)$$

where $S :=]0, T[\times \partial\mathcal{B}$ is the lateral boundary of Q .

Remark 2 We may of course consider Neumann boundary conditions or mixed conditions: this requires additional investigation on the physics. We may also consider \mathbb{R}^n as the domain using appropriate decay properties at infinity instead of the ball: the techniques are quite similar.

We have a generic classical result (see [14] p. 632 for example) which can be sharpened of course. To simplify the presentation, we now assume from now that the sound speed c is equal to 1.

Theorem 4.2 Assume that $u \in L^2(0, T; H^{-1}(\mathcal{B}))$. Then, Equation (12) has a unique solution $y[u] \in L^2(0, T; H_o^1(\mathcal{B})) \cap C^0([0, T]; L^2(\mathcal{B}))$.

In the sequel we denote

$$W := L^2(0, T; H_o^1(\mathcal{B})).$$

Open problem 1 We have set $u(t, x) := u_o(x) \frac{\partial j}{\partial t}(t)$ where j is a smooth approximation of the Dirac measure. This gives the natural regularity of the control function. However, an interesting challenge is to perform the following analysis using less smooth control functions.

4.2 The control problem

Following Scherzer [19] we assume that u has a compact support contained in $[0, T] \times \Omega$, where Ω is a bounded open subset of \mathbb{R}^n containing the support of the object to be recovered. The pressure y is measured (observed) on $\Sigma = [0, T] \times \Gamma$ where $\Gamma \subset \partial\Omega$ is contained (most of time strictly) in $\partial\Omega$. The inverse problem which consists in recovering u from measurements of y on Σ can be formulated as the following minimization problem:

$$\left| \begin{array}{l} \text{Minimize} \quad \int_{\Sigma} (y(u) - y_d)^2 dt d\gamma \\ \text{s.t.} \quad u \in \mathcal{U}, \end{array} \right.$$

where y_d is the measured pressure and \mathcal{U} is the admissible control function space. Many difficulties then arise:

- The problem is known to be ill-posed: we cannot even ensure the existence of a solution. One must add a regularization term for u . A standard way to perform the regularization consists in adding to the functional a Tychonov term:

$$\alpha \int_Q u^2 dx dt \quad \text{with} \quad \alpha > 0,$$

or rather term inspired by the regularization by mollification method

$$\alpha \int_Q (B_\beta u)^2 dx dt$$

where $\alpha > 0$,

$$B_\beta(u) = u - \phi_\beta *_x u, \tag{13}$$

and ϕ_β is defined as in subsection 3.2. Here $*_x$ denotes the spatial convolution (with respect to x). More precisely

$$\int_Q (B_\beta u)^2 dx dt = \int_0^T \int_{\mathcal{B}} (u - \phi_\beta *_x u)^2(x, t) dx dt .$$

Note that $B_\beta = I$ gives the classical Tychonov term.

Open problem 2 *A crucial point is to investigate the physical model and the qualitative properties of the control in order to choose an appropriate regularization term: we may choose the solution with minimal energy, but it may not be the best choice. We choose the above regularization by mollification term for the moment. This choice has to be considered precisely in the future.*

Open problem 3 *A natural question is that of describing the asymptotic behavior of the solution as the regularization parameter α goes to 0 (this is well-known for Tychonov regularization process for example) and perform sensitivity analysis with respect to β .*

- In order to define the observation term in the cost functional, the trace of $y[u]$ on Σ has to belong to $L^2(\Sigma)$. This depends on the regularity of u . However, in the case of point detectors, the observation term would take the form

$$\sum_{i=1}^N \int_{[0,T]} (y[u] - y_d)^2(t, x_i) dt = \sum_{i=1}^N \int_{[0,T] \times \mathbb{R}^n} (y[u] - y_d)^2(t, x) dt d\delta_{x_i}(x),$$

in which $d\delta_{x_i}$ denotes the Dirac measure at x_i . Notice that one may *relax* the above functional and write instead

$$\sum_{i=1}^N \int_{[0,T] \times \mathbb{R}^n} (y[u] - y_d)^2(t, x) dt d\mu_i(x),$$

in which $d\mu_i$ is a relaxed version of $d\delta_{x_i}$, *e.g.* a gaussian measure centered at x_i . Clearly, the *width* of each μ_i should be less than, say, one half of the expected wavelength of the pressure wave, so that the requested fit is physically acceptable.

Open problem 4 *Study the asymptotic behavior of the solution as the fit measures μ_i approach the Dirac measures δ_{x_i} .*

- Even if the cost functional makes sense, using duality methods and integrating by parts is not possible since Γ is not a closed surface (roughly speaking, there is no *inside* and *outside*).

To overcome the last difficulty we regard Γ as the “limit” of a family of open subsets $\omega_\varepsilon : \lim_{\varepsilon \rightarrow 0} \omega_\varepsilon = \Gamma$. This convergence must be clarified of course (using tools from shape optimization, as Γ -convergence for example). A simple way to perform this approximation is to set

$$\omega_\varepsilon = \bigcup_{x \in \Gamma} \mathcal{B}(x, \varepsilon),$$

where $\mathcal{B}(x, \varepsilon)$ is the open ball of radius ε centered at x (see Figure 3).

In the case where there is a finite number of sensors located at $x_i, 1 \leq i \leq N, x_i \in \Gamma$ one may choose

$$\omega_\varepsilon = \bigcup_{i=1}^N \mathcal{B}(x_i, \varepsilon). \quad (14)$$

So, we replace a boundary observation by a distributed observation. We set $\Omega_\varepsilon = \Omega \cup \omega_\varepsilon$ and $\Gamma_\varepsilon = \partial\omega_\varepsilon$.

Open problem 5 • *More generally Ω_ε is defined as a perturbation of Ω : there are many questions related to the asymptotic behavior of the ε -solution as $\varepsilon \rightarrow 0$. One may use tools as the Γ -convergence for example.*

- *Another interesting question is to look for an optimal ω_ε with respect to a criterion given by the experimental setup for example.*

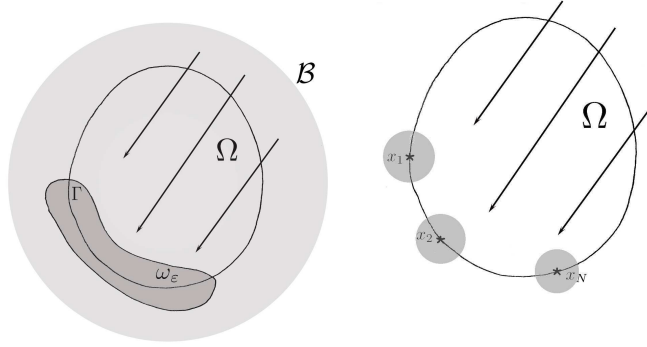


Figure 3: Observation surface relaxation

Finally, the regularized optimal control problem reads:

$$(\mathcal{P}_\varepsilon) \quad \begin{cases} \min J_\varepsilon(y, u) := \frac{1}{2} \int_{[0, T] \times \omega_\varepsilon} (y - y_d)^2(t, x) dt dx + \frac{\alpha}{2} \int_{[0, T] \times \Omega} (B_\beta u)^2(t, x) dt dx \\ y = y[u] \text{ solution to (10), } u \in \mathcal{U} \end{cases}$$

where $\alpha > 0$, $y_d \in L^2(Q)$ and \mathcal{U} is defined for example as

$$\mathcal{U} := \{u \in L^2([0, T] \times \mathcal{B}) \mid u(t, x) = 0 \quad a.e. (t, x) \in]0, T[\times (\mathcal{B} \setminus \Omega)\} .$$

Remark 3 *One can choose*

$$\mathcal{U} := \{u \in L^2([0, T] \times \mathcal{B}) \mid u(t, x) = u_o(x) \frac{\partial j}{\partial t}(t) \quad a.e. (t, x) \in]0, T[\times \Omega, \text{ supp}(u_o) \subset \Omega\} .$$

In the case where the control is an initial one the regularization term could be

$$\frac{\alpha}{2} \int_{\mathcal{B}} (B_\beta u_o)^2(x) dx \left(= \frac{\alpha}{2} \int_{\Omega} (B_\beta u_o)^2(x) dx \right) .$$

Theorem 4.3 *For every $\varepsilon > 0$ problem $(\mathcal{P}_\varepsilon)$ has a unique solution $(y_\varepsilon, u_\varepsilon)$*

Proof.- The proof is standard. □

Open problem 6 *One has to precisely study the asymptotic behavior of $(y_\varepsilon, u_\varepsilon)$ with respect to ε and if possible give error estimates.*

4.3 Optimality conditions

Once the optimal control problem has been formulated it is easy to use the classical machinery (see [24]) introducing the adjoint state p_ε :

$$\begin{cases} \frac{\partial^2 p_\varepsilon}{\partial t^2} - \Delta p_\varepsilon = \begin{cases} y_\varepsilon - y_d & \text{in } [0, T] \times \omega_\varepsilon \\ 0 & \text{elsewhere} \end{cases} \\ p_\varepsilon(T, x) = 0 \text{ in } \mathcal{B}, \\ \frac{\partial p_\varepsilon}{\partial t}(T, x) = 0, \text{ in } \mathcal{B}, \\ p_\varepsilon = 0, \text{ on } S \end{cases}$$

We get the following optimality system

Theorem 4.4 *For every $\varepsilon > 0$ a necessary and sufficient condition for $(y_\varepsilon, u_\varepsilon) \in W \times \mathcal{U}$ to be the solution to $(\mathcal{P}_\varepsilon)$ is*

$$\left\{ \begin{array}{l} \frac{\partial^2 y}{\partial t^2} - \Delta y = u, \text{ in } Q, \\ y(0, x) = 0, \text{ in } \mathcal{B}, \\ \frac{\partial y}{\partial t}(0, x) = 0, \text{ in } \mathcal{B}, \\ y = 0, \text{ on } S \end{array} \right. \quad (15a)$$

$$\left\{ \begin{array}{l} \frac{\partial^2 p_\varepsilon}{\partial t^2} - \Delta p_\varepsilon = \begin{cases} y_\varepsilon - y_d & \text{in } [0, T] \times \omega_\varepsilon \\ 0 & \text{elsewhere} \end{cases} \\ p_\varepsilon(T, x) = 0 \text{ in } \mathcal{B}, \\ \frac{\partial p_\varepsilon}{\partial t}(T, x) = 0, \text{ in } \mathcal{B}, \\ p_\varepsilon = 0, \text{ on } S \end{array} \right. \quad (15b)$$

$$\forall u \in \mathcal{U}, \quad \int_Q (p_\varepsilon + \alpha B_\beta^* B_\beta u_\varepsilon)(u - u_\varepsilon) dt dx \geq 0, \quad (15c)$$

where B_β^* denotes the adjoint operator of B_β . Note that we have embedded the TAT model in a more general class of problems where the control function is no longer “decoupled”. In the (TAT) case where $u(t, x) = f_0(x)f(t)$ we may use the very specific structure of the control function. A similar source identification problem has already been studied for example in [33] in a different framework, where the measured data was the normal derivative.

4.4 The controllability point of view

Another way to consider the problem, which seems to be the most natural one is a controllability approach. Roughly speaking, we look for a control function u with support in $]0, T[\times \Omega$ such that $y[u]$ is given on the set $\Sigma =]0, T[\times \Gamma$. It is clear that the solution is not unique if there is some. However the existence is not obvious both in the cases of exact and approximate controllability. There is a huge literature on controllability/observability theory and we cannot mention all the papers. However, Bardos, Lebeau and Rauch have shown in a famous paper [9] that for the observation or control of solutions of second-order hyperbolic equation a necessary and sufficient condition for controllability is that the region of control meet every ray of geometric optics that has, at worst, transverse reflection at the boundary. More precisely, for multidimensional problems, the region of control must meet each ray in a non diffractive point. This condition is not ensured in our case since the observability (stabilization) region ω_ε is not necessarily connected to the control region Ω .

Open problem 7 *What could be a good choice of ω_ε or Γ to give some existence results for the controllability problem:*

Find u with compact support in Ω such that $y[u] = y_d$ on Γ or ω_ε ?

Which model would be appropriate for using controllability techniques for the wave equation (HUM method, Carleman estimates) ?

5 Numerical experimentation

We now present some numerical simulations to compute a simple TAT model with a closed observation surface (a sphere) and a constant sound speed $c \equiv 1$. More precisely we want to recover the source u_0 which drives the following equation

$$\begin{cases} \left(\frac{\partial^2 y}{\partial t^2} - \Delta y \right) (t, x) = 0, & (t, x) \in [0, T] \times \Omega, \\ y(t, x) = 0, & (t, x) \in [0, T] \times \partial\Omega, \\ y(0, x) = u_0, \quad \frac{\partial y}{\partial t}(0, x) = 0, & x \in \Omega \end{cases} \quad (16)$$

from measurements y_{obs} on the boundary of Ω . Here Ω is the 0-centered ball of radius 1. Thanks to symmetry we reduce the problem to a 2D problem.

We investigate three methods

- The basic filtered back-projection method;
- The Time Reversal method;
- The resolution of system (15) with a conjugate-gradient method.

These methods have been tested using Shepp-logan phantom. To perform a rough comparison, we do not use the recent improvement of these methods (see for example [19, 6, 7, 31]). In that spirit we do not compare precisely the convergence speeds and the CPU run time, since we have not used optimized codes and methods.

Note that we have chosen an experimental setting where the comparison of these techniques was relevant (constant sound speed and closed observation surface).

5.1 The filtered back-projection

The filtered back-projection (FBP) method remains one of the most commonly used techniques to invert integral operators such as the classical Radon transform or the spherical Radon transform R , for it provides an exact inversion formula in some specific acquisition geometries. Concerning the thermo-acoustic tomography, since these formulae allow the inversion of the spherical Radon transform, they require the strongest approximation we have discussed: a constant speed of sound, a perfect Dirac pulse and a complete data set (most of the time, a whole sphere).

The first known FBP formula was derived in [16] for odd dimensions. Later on, in [19], the authors used the approximate inverse concept to regularize this formula. Here, we implement an algorithm proposed by Finch in [15] for the two-dimensional case, which is based on the closed formula:

$$f(x) = \frac{1}{2\pi} \int_{S^1} \int_0^2 \partial r (r \partial r R_{2d})(\omega, r) \log |r^2 - |x - \omega|^2| \, dr ds(\omega),$$

for smooth functions f supported in the unit ball. The derivations are approximated with symmetric finite differences and the numerical integrations are performed by means of linear interpolations and of the trapezoidal rule. This algorithm is very efficient and quite stable when one deals with a sufficiently large amount of detectors (Figures 5 and 7). Nevertheless, the implementation becomes unstable when the angular sampling of the detectors around the unit circle doesn't allow the trapezoidal rule to be accurate (Figure 8).

5.2 Time reversal

The idea of this method is the following (see [20]): thanks to the Huygens' principle (in odd dimension), the wave leaves the unit disc in a finite time, such that there exists a time T such that

the pressure vanishes for any $t \geq T$. Consequently, as the wave standard equation is reversible, we may solve the backward problem starting from time T with boundary conditions equal to the measured data to recover the initial condition. This method has been adapted to the case where space dimension is even (see [31]) and in attenuating acoustic media [6, 7]. The backward problem was computed with a classical finite differences scheme.

5.3 The control approach

There are many classical tools to make this algorithm converge (splitting, relaxation). The more delicate part is the computation of $\Pi_{\mathcal{U}}$ since the support constraint is a pointwise constraint and we perform a L^2 -projection. An alternative is to keep the constraint as a control constraint and deal with the associate Lagrange multiplier. This will be addressed in future work.

Nevertheless, in a linear framework, Problem $(\mathcal{P}_\varepsilon)$ reduces to:

$$(\mathcal{P}_\varepsilon) \quad \begin{cases} \min \frac{1}{2} \|Wu - y_d\|_{L^2([0,T] \times \omega_\varepsilon)}^2 + \frac{\alpha}{2} \|B_\beta u\|_{L^2([0,T] \times \Omega)}^2 \\ u \in L^2([0, T] \times \Omega), \end{cases}$$

where the linear operator W is defined by $Wu := y[u]$, so that the optimality condition (15c) reads:

$$(W^*W + \alpha B_\beta^* B_\beta)u_\varepsilon = W^*y_d. \quad (17)$$

Here, B_β is defined by (13) and the kernel ϕ_β is a gaussian function with standard deviation $\beta \approx 3.10^{-3}$. We have set $\alpha = 0.4$. Finally, ω_ε is given by (14), where ε is set to a single pixel size.

Since the self-adjoint operator $W^*W + \alpha B_\beta^* B_\beta$ is positive definite, we chose to solve Equation (17) by means of the conjugate gradient algorithm. It is straightforward that W^*Wu_ε is nothing but the solution p_ε of Equation (15b) with y_d replaced by 0. Moreover, W^*y_d is obtained as the solution of Equation (15b) with $y_\varepsilon - y_d$ replaced by y_d . The forward and backward problems (15a) and (15b) are solved by means of a leapfrog discretization scheme on a staggered grid.

In order to avoid handling large grids (due to the size of \mathcal{B}), we use an appropriate PML (Perfectly Matched Layer) technique (see [10]).

5.4 Numerical tests

Each method is tested on the Shepp-Logan phantom:



Figure 4: The Shepp-Logan phantom (256×256 pixels).

We investigate the cases where

- data are not corrupted;
- a white gaussian noise (SNR=0.15) is added to the simulated data;
- the number of detectors is either 50 or 360 (with a uniform angular sampling on the whole circle).



Figure 5: Noiseless data, 360 detectors. Left: filtered back-projection solution. Center: time reversal solution. Right: control approach solution.

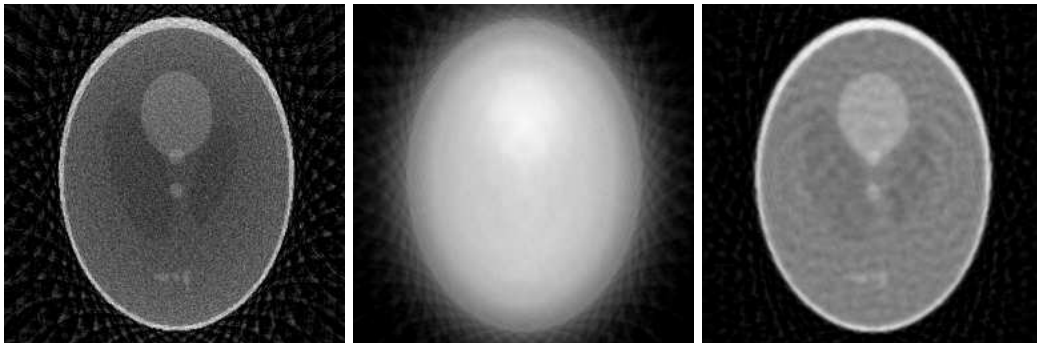


Figure 6: Noiseless data, 50 detectors. Left: filtered back-projection solution. Center: time reversal solution. Right: control approach solution.



Figure 7: Noisy data, 360 detectors. Left: filtered back-projection solution. Center: time reversal solution. Right: control approach solution.

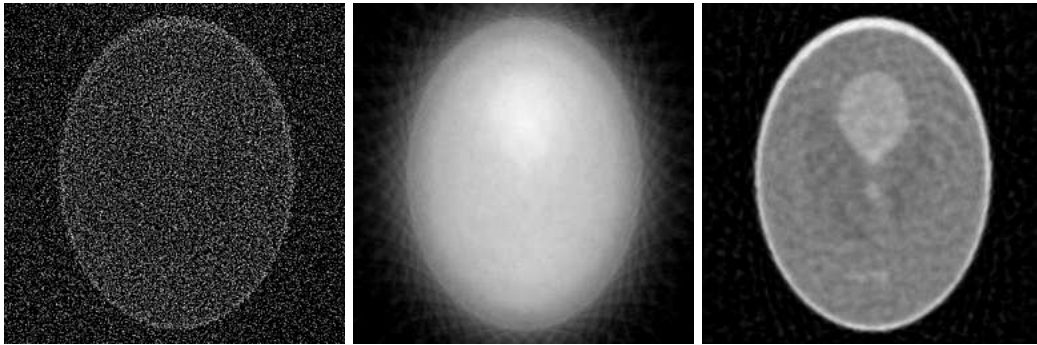


Figure 8: Noisy data, 50 detectors. Left: filtered back-projection solution. Center: time reversal solution. Right: control approach solution.

Influence of the mollification

In order to show the relevance of the chosen regularization process, we present thereafter the solutions obtained with the control approach for $\alpha = 0$ and $\alpha = 0.4$. If $\alpha = 0$, the existence of a solution of Problem $(\mathcal{P}_\varepsilon)$ is not ensured. However, it has been possible to compute a minimizing sequence. The solutions presented in Figure 9 are obtained with 20 iterations of a conjugate gradient algorithm.

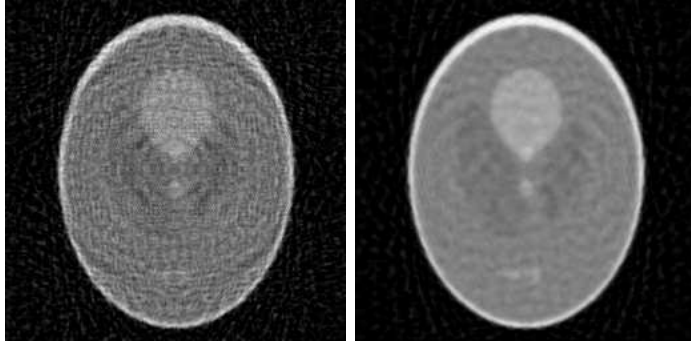


Figure 9: Left (resp. Right): control approach solution without (resp. with) regularization – noiseless data, 50 detectors.

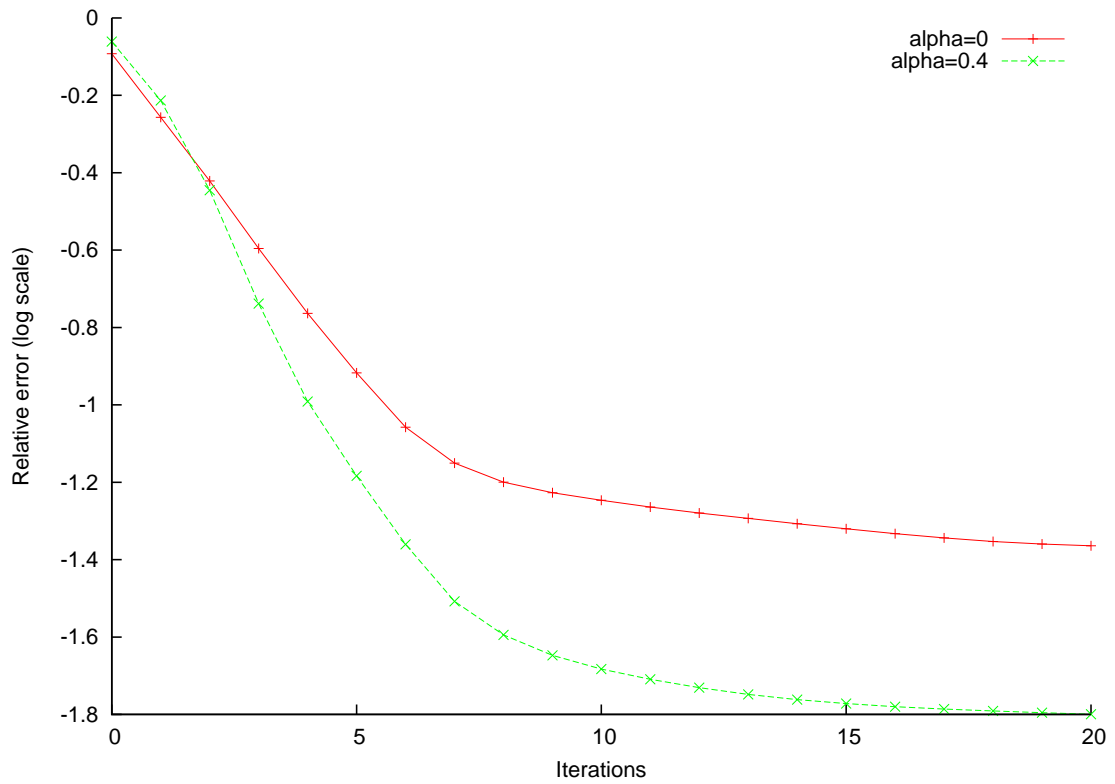


Figure 10: Convergence rates for $\alpha = 0$ (continuous line) and $\alpha = 0.4$ (dashed line)- The relative error is computed as $\|u_c - u_{orig}\|_2 / \|u_{orig}\|_2$ where u_c is the computed solution and u_{orig} the (original) object to recover.

6 Conclusion

We hope we have clearly presented many open questions about a challenging imaging process. We can apply these remarks to photo-acoustic tomography (PAT) as well: the equations are the same (wave equation related to acoustic part) but the frequency scale is different. There are many others questions that arise as for example the optimal location of sensors (shape-optimization problem), variable speed sound and/or non linear equations, filtering effect on u and so on.

The numerical tests we have presented are to be performed with more accuracy. Indeed, the sensitivity to parameters (α, β) has to be deeply investigated. Moreover, it is known that for time semi-discrete systems, due to high frequency spurious components, the exponential decay property may be lost as the time step tends to zero (see Zuazua [34, 35]) so that numerical schemes are highly unstable. In [17], Ervedoza and Zuazua use a decoupling argument of low and high frequencies, the low frequency observability property for time semi-discrete approximations of conservative linear systems and the dissipativity of the numerical viscosity on the high frequency components. All these questions will be discussed in a future work.

References

- [1] (MR2482153) N. Alibaud, P. Maréchal & Y. Saesor, *A variational approach to the inversion of truncated Fourier operators*, Inverse Problems **25** (2009), no 4, .
- [2] N. Alibaud, X. Bonnefond & P. Maréchal, *Analyse asymptotique de la régularisation par mollification*, Actes du colloque: Mathématiques pour l'image, Presses Universitaires d'Orléans (2009).
- [3] (MR2736968) H. Ammari, E. Bossy, V. Jugnon, & H. Kang, *Mathematical modeling in photoacoustic imaging of small absorbers*. SIAM Rev. **52** (2010), no. 4, 677–695
- [4] (MR2677808) H. Ammari, P. Garapon, L. Guadarrama Bustos & H. Kang *Transient anomaly imaging by the acoustic radiation force*. J. Differential Equations 249 (2010), no. 7, 1579–1595
- [5] H. Ammari, J. Garnier, V. Jugnon, & H. Kang, *Direct reconstruction methods in ultrasound imaging*. Chapter in a Lecture Notes in Mathematics Volume, Springer-Verlag, 2011
- [6] H. Ammari, E. Bretin, V. Jugnon, & A. Wahab, *Photo-acoustic imaging for attenuating acoustic media*. Chapter in a Lecture Notes in Mathematics Volume, Springer-Verlag, 2011
- [7] H. Ammari, E. Bretin, J. Garnier, & A. Wahab, *Time reversal in attenuating acoustic media*. to appear in Contemporary Mathematics, 2011
- [8] (MR2440996) M.A Anastasio, J.Zhang, D. Modgil and P.J La Rivière, *Application of inverse source concepts to photoacoustic tomography*, Inverse Problems **23** (2007), no. 6, 21–35
- [9] (MR1178650) C. Bardos, G. Lebeau and J. Rauch, *Sharp Sufficient Conditions for the Observation, Control, and Stabilization of Waves from the Boundary*, SIAM J. Control Optim. **30** (1992), Issue 5, 1024–1065
- [10] J. P. Berenger, *A perfectly matched layer for the absorption of electromagnetic waves*, J. Comput. Phys., pp. 185-200, Oct. 1994.
- [11] (MR2489931) X. Bonnefond and P. Maréchal, *A variational approach to the inversion of some compact operators*, Pacific Journal of Optimization, **5(1)** (2009) 97-110.
- [12] (MR2601332) F. Boyer, F. Hubert and J. Le Rousseau, *Discrete Carleman estimates for elliptic operators and uniform controllability of semi-discretized parabolic equations*, J. Math. Pures Appl. (9) **93** (2010), no. 3, 240–276

- [13] (MR2440999) P. Burgholzer, J. Bauer-Marschallinger, H. Grün, M. Haltmeier and G. Paltauf, *Temporal back-projection algorithms for photoacoustic tomography with integrating line detectors*, Inverse Problems **23** (2007), no. 6, 65–80
- [14] (MR0792484) R. Dautray and J.L. Lions, “Analyse mathématique et calcul numérique pour les sciences et les techniques.”, Masson, Paris, 1987
- [15] (MR2366991) D. Finch, M. Haltmeier and R. Rakesh, *Inversion of spherical means and the wave equation in even dimensions*, SIAM J. Appl. Math. **68**, (2007), no. 2, 392–412
- [16] (MR2050199) D. Finch, S. Patch and R. Rakesh, *Determining a function from its mean values over a family of spheres*, SIAM J. Math. Anal. **35**, (2004), 1213–40
- [17] (MR2487899) S. Ervedoza and E. Zuazua, *Uniformly exponentially stable approximations for a class of damped systems*, J. Math. Pures Appl., **91**, (2009), no. 1, 20–48 **68**
- [18] (MR2535737) M. Gugat, A. Keimer and G. Leugering, *Optimal distributed control of the wave equation subject to state constraints*, Z. Angew. Math. Mech. **89**, (2009) , 420 – 444
- [19] (MR2170772) M. Haltmeier, T. Schuster and O. Scherzer, *Filtered backprojection for thermoacoustic computed tomography in spherical geometry*, Math. Meth. Appl. Sci. **28**,(2005), no. 16, 1919–1937
- [20] (MR2438941) Y. Hristova, P. Kuchment and L.Nguyen, *Reconstruction and time reversal in thermoacoustic tomography in acoustically homogeneous and inhomogeneous media*, Inverse Problems, **24**, (2008), no.5, 055006, 25 pp.
- [21] (MR2501026) Y. Hristova, *Time reversal in thermoacoustic tomography—an error estimate*, Inverse Problems, **25**, (2009), no. 5, 055008, 14 pp.
- [22] (MR2438956) L. A. Kunyansky, *Thermoacoustic tomography with detectors on an open curve: an efficient reconstruction algorithm*, Inverse Problems, **24** , (2008), no. 5, 055021, 18 pp.
- [23] (MR0969968) A. Lannes, S. Roques and M.-J. Casanove, *Stabilized reconstruction in signal and image processing; Part I: partial deconvolution and spectral extrapolation with limited field*, J. Mod. Opt. **34**, (1987), 161-226.
- [24] (MR0244606) J.L. Lions, “Contrôle optimal de systèmes gouvernés par des équations aux dérivées partielles”, Dunod, Paris, 1968
- [25] (MR0247243) J.L. Lions and E. Magenes, “Problèmes aux limites non homogènes”, Dunod, Paris, 1968
- [26] (MR1057035) A.K. Louis and P. Maaß, *A mollifier method for linear operator equations of the first kind*, Inverse Problems **6**, (1990), 427–440.
- [27] (MR1382237) A.K. Louis, *Approximate inverse for linear and some nonlinear problems*, Inverse Problems **12**, (1996), 175–190.
- [28] (MR1684469) A.K. Louis, *A unified approach to regularization methods for linear ill-posed problems* Inverse Problems **15**, (1999), 489–498.
- [29] (MR2440994) S. K Patch and O.Scherzer, *Photo- and Thermo-Acoustic Imaging Introduction*, Inverse Problems, **23**, (2007), no. 6, 1–10
- [30] (MR2455620) O. Scherzer, M. Grasmair, H. Grossauer, M. Haltmeier and F. Lenzen, “Variational Methods in Imaging”, Springer, 2008

- [31] J.Qian, P. Stefanov, G. Uhlmann and H. Zhao, *An efficient Neumann-series based algorithm for Thermoacoustic and Photoacoustic Tomography with variable sound speed* (with), to appear in SIAM J. Imaging Sciences, (2011).
- [32] (MR2519863) P. Stefanov and G.Uhlmann, *Thermoacoustic tomography with variable sound speed*, Inverse Problems, **25** (2009), no. 7, 075011, 16 pp.
- [33] (MR1324655) M. Yamamoto, *Stability, reconstruction formula and regularization for an inverse source hyperbolic problem by a control method*, Inverse Problems, **11** (1995), 481-496.
- [34] (MR1897693) E. Zuazua, *Controllability of partial differential equations and its semi-discrete approximations*, Discrete Continuous Dynam. Systems, **8**, (2002), no. 2, 469–513.
- [35] (MR2179896) E. Zuazua, *Propagation, Observation, and Control of Waves Approximated by Finite Difference Methods*, SIAM Review, 2005, **47** (2005) , no. 2, 197–243